Int. J. Heat Mass Transfer. Vol. 33, No. 12, pp. 2641–2649, 1990
Printed in Great Britain

0017-9310/90 $3.00 + 0.00

Effect of thermocouple sensor dynamics on surface heat flux predictions obtained via inverse heat transfer analysis

KEITH A. WOODBURY
Department of Mechanical Engineering, The University of Alabama, Tuscaloosa, AL 35487-0276, U.S.A.

(*Received* 7 *April* 1989 *and in final form* 2 *February* 1990)

Abstract—A simple thermocouple model is used in this paper to generate data by simulating the imposition of a triangular heat flux history on a one-dimensional domain. A general inverse heat conduction (IHC) analysis computer program is developed and used to estimate the heat flux history based on the generated data. The results show that the effect of the thermocouple's time constant is to diminish the magnitude of the predicted heat flux history and displace its distribution in time.

1. INTRODUCTION

INVERSE methods have gained popularity over the last 20 years in many fields [1–4] including heat transfer [5–9]. In the heat transfer arena, these methodologies are used extensively to provide estimates of the surface heat transfer based on temperature measurements from the body's interior. This contrasts the 'normal' task of the heat transfer analyst which is to provide predictions of a body's internal temperature *given* the external variation in surface heat flux. For this reason, these techniques are referred to as inverse heat conduction (IHC) methods.

Estimation of surface heat fluxes by application of inverse methodologies is gaining acceptance as a *bona fide* technique for obtaining transient heat flux data. Although any available temperature sensor may be employed to provide the internal temperature history of the body, the thermocouple is the most commonly used. When the heat flux is steady, or varying only slowly in time, application of the IHC analysis yields accurate values for the unknown flux. However, if the heat flux is changing rapidly, even in a non-periodic manner, the effect of inherent thermocouple sensor dynamics is to corrupt the temperature history in a deterministic way. If this data is then used to estimate the unknown surface heat flux, errors in both magnitude and timing of the heat flux history will result.

A thermocouple is a junction of two dissimilar metals which produces an electromotive force (EMF) which is proportional to the temperature of the junction. Such a device accurately represents its own temperature quite well, and its ability to portray the transient temperature of its surroundings depends on two significant factors. First, as the body's temperature changes, there must be heat transfer between the body and the sensor, in order for the sensor to follow the body's temperature. In order to achieve accurate readings, then, the contact resistance between the body and the sensor must be minimized.

Secondly, the thermocouple junction inherently has a finite volume, and this volume's thermal mass must change temperature as rapidly as possible to mirror the change in the body's temperature. Therefore, for a given thermocouple material, the mass of the junction should be minimized in order to attain a rapid thermocouple response. Attention to these details in a thermocouple's construction and installation will minimize the thermocouple's dynamics; however, they cannot be eliminated completely.

This scenario begs the question: 'What are the effects of inherent thermocouple sensor dynamics on estimates of transient heat fluxes if IHC methods are employed?' This is the central question of this paper and has relevance in physical situations where temperatures and fluxes are changing rapidly, such as quenching or ablative heating.

What follows in this paper is a description of the current implementation of the IHC method, which is a generalization of the function specification method of Beck [5, 10]. Next, a simple thermocouple model is presented which is used to generate data from thermocouples with different time constants. Finally, the central question is addressed by applying the IHC method to the data generated from the thermocouple model and examining the results. A suggestion for compensating the IHC algorithm for the thermocouple's time constant is made before the conclusion of this paper.

2. CURRENT IHC ALGORITHM

The IHC algorithm developed for this study is a generalization of the function specification method of Beck [5, 10]. It was desired that the method be as general as possible, so that further modifications could be made to extend its applicability to a wider class of problems. The major aspect of the current method is the segregation of the thermal model and

NOMENCLATURE

A	surface area [m^2]
$[A]$, $[B]$	coefficient matrices
a_{ij}	sensitivity of variable i on parameter j
c_p	thermocouple bead constant pressure specific heat [kJ kg^{-1} K^{-1}]
f^+	arbitrary function [dimensional]
f	arbitrary function [dimensionless]
h	heat transfer coefficient [W m^{-2} K^{-1}]
k	thermal conductivity [W m^{-1} K^{-1}]
L	reference length [m]
n	number of observations
P	model parameter
$q^{+\prime\prime}$	heat flux [W m^{-2}]
$\dot{q}''_{\text{ref}}$	reference heat flux [W m^{-2}]
$\dot{q}''$	dimensionless heat flux, $q^{+\prime\prime}/\dot{q}''_{\text{ref}}$
r	number of future time steps
s	number of sensors
S	sum of squares of deviations
t^+	time [s]
t	dimensionless time, $t^+\alpha/L^2$
T^+	temperature [K]
T_b^+	thermocouple bead temperature [K]
T_∞^+	thermocouple environment temperature [K]
T	dimensionless temperature, $(T^+ - T_{\text{ref}})/\dot{q}''_{\text{ref}}(L/k)$
V	volume [m^3]
w_{ij}	weighting factor (equation (9))
x^+	distance coordinate [m]
x	dimensionless distance, x^+/L
$\hat{y}_i$	model-computed value of y
$\tilde{y}_i$	experimentally observed value of y.

Greek symbols

α	material thermal diffusivity [m^2 s^{-1}]
ρ	thermocouple bead density [kg m^{-3}]
τ^+	time constant [s]
τ	dimensionless time constant, $\tau^+\alpha/L^2$.

the non-linear estimation procedures in the algorithm. In this way, extensions to higher dimensions or inclusion of effects such as solidification can be made by modifying only the thermal model. A general description of the current IHC algorithm will be given, followed by a validation of the implementation's method.

2.1. *Description of the algorithm*

The thermal model employed in the current IHC algorithm is restricted to one-dimensional Cartesian systems with constant thermal properties. The governing differential equation for such a system is

$$\frac{1}{\alpha}\frac{\partial T^+}{\partial t^+} = \frac{\partial^2 T^+}{\partial x^{+2}} \tag{1}$$

subject to the boundary conditions

$$q^{+\prime\prime}(0,t^+) = -k\left.\frac{\partial T^+}{\partial x^+}\right|_{0,t^+} = f_1^+(t^+) \tag{2a}$$

$$q^{+\prime\prime}(L,t^+) = -k\left.\frac{\partial T^+}{\partial x^+}\right|_{L,t^+} = f_2^+(t^+) \tag{2b}$$

and the initial condition

$$T^+(x^+,0) = f_3^+(x^+). \tag{3}$$

These relations can be cast into non-dimensional form by defining the following dimensionless parameters:

$$t = t^+\alpha/L^2, \quad x = x^+/L$$

$$\dot{q}'' = q^{+\prime\prime}/\dot{q}''_{\text{ref}}, \; T = (T^+ - T_{\text{ref}})/\dot{q}''_{\text{ref}}(L/k). \tag{4}$$

Then equations (1)–(3) become

$$\frac{\partial T}{\partial t} = \frac{\partial^2 T}{\partial x^2} \tag{5}$$

$$\dot{q}''(0,t) = -\left.\frac{\partial T}{\partial x}\right|_{0,t} = f_1^+(t^+)/\dot{q}''_{\text{ref}} = f_1(t) \tag{6a}$$

$$\dot{q}''(1,t) = -\left.\frac{\partial T}{\partial x}\right|_{1,t} = f_2^+(t^+)/\dot{q}''_{\text{ref}} = f_2(t) \tag{6b}$$

$$T(x,0) = (f_3^+(x^+) - T_{\text{ref}})/\dot{q}''_{\text{ref}}(L/k) = f_3(x). \tag{7}$$

In the IHC algorithm, the initial condition $f_3(x)$ in equation (7), which is often a constant value, must be known a priori. However, determination of the heat flux boundary conditions at one or both ends of the domain (equation (6)) is the objective of the IHC method. One or both of these fluxes can be obtained by the current algorithm, if sufficient data are available. This will be discussed below in detail.

In order to provide the predictions of the unknown heat flux, a non-linear estimation method is necessary. The method incorporated in the current algorithm is an iterative least-squares differential correction algorithm [11, 12]. The objective function for the minimization is the sum of the squares of the difference between a model-produced estimate $\hat{y}$ and its corresponding measured value resulting from a physical experiment $\tilde{y}$. That is, a system model is available which yields estimates of the measured values given current values of the unknown parameters

$$\hat{y}_i = F(P_1, P_2, \ldots, P_m, t_i). \tag{8}$$

Here the P's represent the unknown parameters in the system model. The objective function to be minimized can be expressed as

$$S = \sum_{j=1}^{n} \sum_{i=1}^{n} (\hat{y}_i - \tilde{y}_i) w_{ij} (\hat{y}_j - \tilde{y}_j) \quad (9)$$

where n corresponds to the number of measurements that are to be matched. Also, w_{ij} is a weighting factor which becomes necessary when parameters to be estimated have different statistical variance.

It should be noted that, in order to minimize equation (9) with respect to the unknown parameters, the sensitivity matrix embodying the dependence of the system model on the unknown parameters must be determined. This sensitivity matrix is the set of first derivatives of the system model with respect to the unknown parameters. In the non-linear estimation algorithm employed here, this is not done explicitly. Rather, the evaluation of the partial derivatives is performed numerically. Thus, the sensitivity coefficients are computed from a central difference approximation as

$$a_{ij} = \frac{\partial \hat{y}_i}{\partial P_j} \approx \frac{F(P_1, \ldots, P_j + \delta P_j, \ldots, P_m, t_i) - F(P_1, \ldots, P_j - \delta P_j, \ldots, P_m, t_i)}{2\delta P_j}. \quad (10)$$

The minimization algorithm used in the current IHC method is perfectly general in that any model may be used to produce the estimates. The system model can be any combination of mathematical operations required to produce estimates of the measured values. The required sensitivity matrix is computed numerically and the potential complexity of the system model itself poses no limitation on the class of thermal models which may be analyzed.

In the specific case of the estimation of unknown surface heat fluxes, the system model is the differential equation (5) and the unknown parameters are the heat fluxes in equation (6). The measurements $\tilde{y}_j$ in equation (9) become the discrete thermocouple readings $\tilde{T}_j$. This problem is, however, significantly different from the classical parameter estimation problem, since the 'parameters' to be estimated are functions of time. This is what Beck *et al.* [9, 10], call *function estimation*. This can be handled in the context of the current estimation procedure in at least three ways (p. 37 of ref. [10]): (1) consider each time step a new problem with no knowledge of the future, (2) consider each time step a new problem, but realize knowledge of a few future time steps, or (3) consider the whole time domain. The first of these is the classic method of Stoltz, which suffers from numerical instability for small time steps. The last option is computationally inefficient, requiring rather large computer memory to solve a modest problem. The second approach is the one implemented in the current IHC algorithm and is essentially the sequential function specification method espoused by Beck [5, 10].

To apply the IHC method, the partial differential equation (5) must be discretized into an algebraic form. This discretization may be done in many ways (finite difference, finite volume, finite element, implicit, explicit, Crank–Nicolson, Galerkin, etc.) but may be represented algebraically as a matrix equation

$$[A]\{T^{i+1}\} = [B]\{T^{i}\} + \{q^{j}\} \quad (11)$$

where the superscript 'i' is the current time t_i, '$i+1$' is the next time t_{i+1}, and the superscript 'j' may be either 'i', '$i+1$', or '$i+\frac{1}{2}$' according to whether explicit, implicit, or Crank–Nicolson time discretization is employed. The vector $\{q^j\}$ contains the unknown heat fluxes, and for a one-dimensional analysis can contain at most two values.

In the current IHC thermal model, a finite volume spatial discretization is employed, and a fully implicit time discretization is used. The implicit form of the temporal discretization was found by experience to be less sensitive to numerical instability (see Section 2.2 below). Thus, in equation (11), the matrix $[A]$ has a tridiagonal form, $[B]$ is a diagonal matrix, and the index 'j' is equal to '$i+1$'.

The spatial domain must be subdivided to compute the temperature distribution at each time step. The spatial domain may, if desired, be subdivided into nodes of unequal volume, although equal increments are normally chosen. The number of computation points is arbitrary, but must be chosen such that a smooth and reasonable spatial temperature variation results. The only strict requirement is that the actual location of the sensor(s) used must correspond exactly to the location of the analogous computational node.

In the sequential function specification procedure, a functional form for the temporal variation in surface heat flux is assumed. The current IHC implementation follows the choice by Beck *et al.* [10] of the simplest possible function, the constant function. That is, over each computational time interval Δt, the surface heat flux q^j is assumed to remain constant. Then, that constant value of q^j is *temporarily* assumed to remain constant over the next r future time steps. Future time steps are included in the procedure to provide a stabilizing effect on the predictions (p. 125 of ref. [10]). The value of r is also an input variable into the IHC algorithm and is easily changed. The number of measurements to be 'matched' in the sense of equation (9) is $n = r \times s$, where s is the number of sensors employed.

Use of multiple sensors is recommended by Beck (pp. 230–232 of ref. [10]). However, difficulties arise with multiple sensors in a one-dimensional problem estimating a single heat flux. This is because the unknown heat flux will have the highest sensitivity to the sensor closest to that surface. This will require the use of a weighting scheme, so that data from those sensors more remote from the surface will be heeded.

On the other hand, if heat fluxes on *both* ends of a one-dimensional domain are to be estimated, at least two sensors *must* be employed (one corresponding to each surface). Otherwise, an infinite combination of heat fluxes at the two surfaces could account for the change in temperature of the single sensor. What

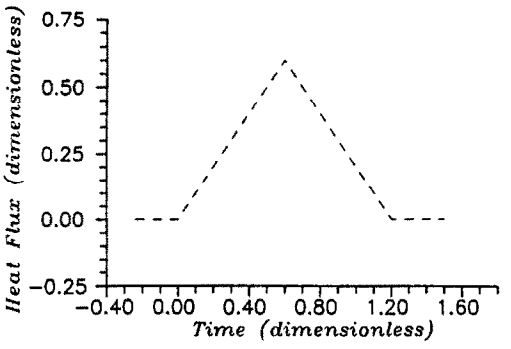

FIG. 1. Triangular heat flux.

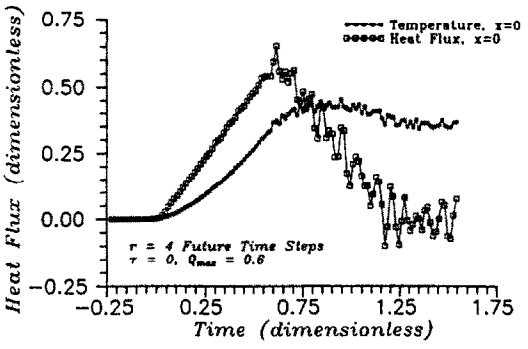

FIG. 3. IHC results using Crank–Nicolson formulation and $r = 4$ future time steps.

results is the flux at the surface which is closest to the sensor will have the highest sensitivity to the measurement. Consequently, that flux will be estimated, and the second surface will be estimated as adiabatic. Correct estimates for the two unknown fluxes will not be obtained.

The current IHC has been verified by comparison to the triangular heat flux test case presented in ref. [10]. The results of this verification are presented in the following section.

2.2. *Algorithm verification*

In order to demonstrate the soundness of the current method, it is applied to an academic case presented by Beck *et al.* (p. 169 of ref. [10]). The case involves the imposition of a triangular heat flux on one end of a domain while the other end remains insulated. The triangular heat flux is depicted in Fig. 1.

Calculations are performed in dimensionless form. Data were generated for a sensor located at the insulated boundary at $x^+ = L$ ($x = 1$). The time interval between the data points was 0.015 (dimensionless time). This temperature history was then input into the IHC algorithm to obtain the estimate of the heat flux history at the surface.

The results of the IHC prediction are shown in Fig. 2 using $r = 4$ future time steps per estimate. These results were obtained using the implicit time discretization as described in the previous section. For comparison, the results of the IHC algorithm using a Crank–Nicolson time discretization are shown in Fig. 3. These results were also obtained using $r = 4$ future time steps per estimate. For both estimations, the time step for the simulation in the thermal portion of the IHC algorithm was identical to the time step in the data (0.015). Notice that, although the results from the implicit formulation in Fig. 2 are not completely smooth, the corresponding results from use of the Crank–Nicolson discretization in Fig. 3 are highly erratic once the time rate of change of the heat flux $d\dot{q}''/dt$ has reversed sign. For this reason, the fully implicit formulation was embraced and adopted for all subsequent computations.

The lack of smoothness in the results of Fig. 2 was not satisfactory. Hence subsequent re-estimates were made to determine the number of future time steps required to yield a smooth result. The IHC algorithm was re-executed using values of $r = 6$ and 8 future time steps. The results for $r = 6$ (not shown) still have a small amount of oscillation in the results after the change in sign of the heat flux time derivative. However, the results for $r = 8$ future time steps, shown in Fig. 4, shows that the results for this case are satisfactorily smooth. The time step again equalled that of the data (0.015), however, in Fig. 4 *and in*

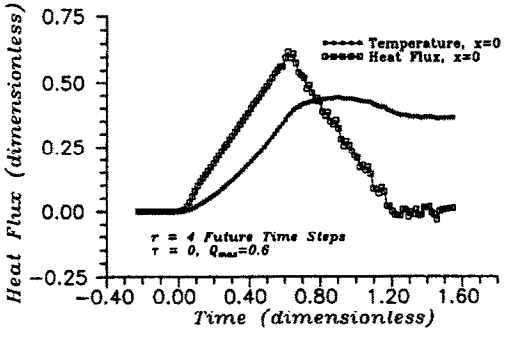

FIG. 2. IHC results using implicit formulation and $r = 4$ future time steps.

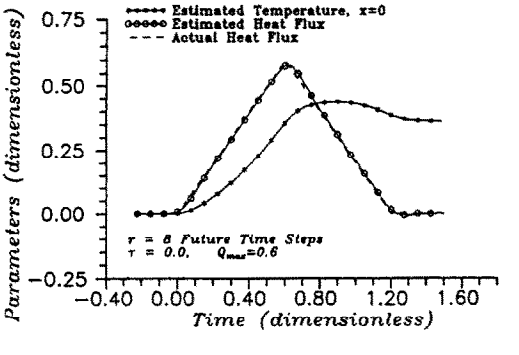

FIG. 4. IHC results using implicit formulation and $r = 8$ future time steps.

Table 1. Calculated heat fluxes at certain times for the triangular heat flux example using the function specification method

t	Exact	$r = 8$ Current method	$r = 4$ (ref. [10])
0.15	0.15	0.141	—
0.51	0.51	0.502	0.5038
0.57	0.57	0.559	0.5347
0.60	0.60	0.578	—
0.63	0.57	0.578	0.5327
0.69	0.51	0.533	0.5018
1.05	0.15	0.157	—

subsequent figures not all computational points are indicated with symbols.

Table 1 shows a comparison of a few specific data points from the estimation procedure to the corresponding exact values. Also shown in Table 1 are the values reported in ref. [10] (Table 5.5, p. 183) for their estimates for this case. The comparison of the quality of the results from the current method to those from ref. [10] is highly favorable.

3. THERMOCOUPLE SENSOR DYNAMICS

As mentioned previously, two major factors require that a thermocouple sensor's indicated temperature lag behind the actual temperature the sensor is attempting to indicate. These factors are (1) contact resistance between the sensor and the body and (2) the thermal mass of the thermocouple junction. In this section a brief description of the simplest thermocouple sensor model will be given, along with a demonstration of this model's effect on the indicated temperature.

3.1. *The simplest model*

The simplest model for a thermocouple involves incorporation of the two factors mentioned above—contact resistance and thermal mass. Such a model neglects other possibly important factors such as heat loss and temperature gradients along the leads.

The thermocouple model is shown in Fig. 5. The thermal resistance is depicted as $R_{th} = 1/hA$, where h is the heat transfer coefficient between the thermocouple bead and the surrounding medium and A the surface area of the bead. In situations of interest in the present investigation, this h would *not* be a convection coefficient but would represent the effect of an air gap or some otherwise imperfect thermal contact between the thermocouple and the surrounding solid medium.

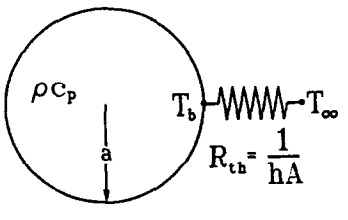

FIG. 5. Thermocouple model and parameters.

The assumptions of a homogeneous thermocouple bead with constant thermal properties and uniform contact resistance are made. With the further assumption of negligible internal temperature gradients within the bead, an energy balance leads to the differential equation governing the temperature of the bead as a function of time as

$$\frac{dT_b^+}{dt^+} = \frac{q^+}{\rho c_p} = \frac{hA}{\rho c_p V}(T_\infty^+(t^+) - T_b^+) = \frac{1}{\tau^+}(T_\infty^+(t^+) - T_b^+) \quad (12)$$

which is subject to the initial condition

$$T_b^+(0) = T_0^+. \quad (13)$$

In dimensionless form these equations become

$$\frac{dT_b}{dt} = \frac{1}{\tau}(T_\infty(t) - T_b) \quad (14)$$

and

$$T_b(0) = (T_0^+ - T_{ref})/\dot{q}''_{ref}(L/k) = T_0. \quad (15)$$

The two factors controlling the thermocouple's response are seen to combine as a ratio into a single parameter τ^+. This parameter is often referred to as the *time constant* and has units of time (s). Two important observations regarding the nature of equation (14) are (1) the equation is intractable at present since the temperature of the surrounding medium $T_\infty(t)$ is an unspecified function of time and (2) the parameter τ, although assumed constant in this formulation, may in fact change with time and/or temperature.

3.2. *Effect of τ on sensor temperature*

A solution for the thermocouple's response can be computed if the temperature history of the surrounding medium $T_\infty(t)$ in equation (14) is known. A parametric investigation was undertaken to determine the effect of the time constant τ on the sensor's indicated temperature.

A one-dimensional domain insulated at $x^+ = L$ ($x = 1$) was simulated numerically using the triangular heat flux shown in Fig. 1 as the boundary condition at $x^+ = 0$ ($x = 0$). A thermocouple located at $x = 1$ was simulated by including the sensor dynamics depicted by equation (14) and using the value of the temperature of the body at $x = 1$ as the time varying T_∞. The temperature of the body was determined from a Crank–Nicolson numerical procedure. The temperature of the sensor was determined at each time step using a fully implicit numerical differencing scheme.

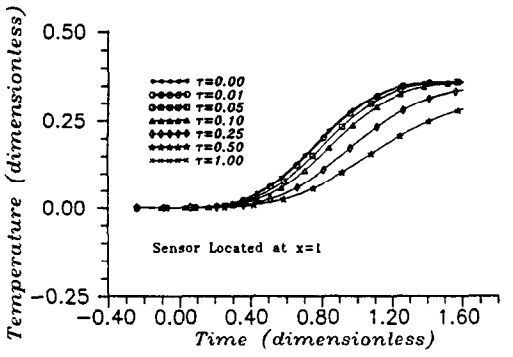

FIG. 6. Effect of τ on sensor temperature.

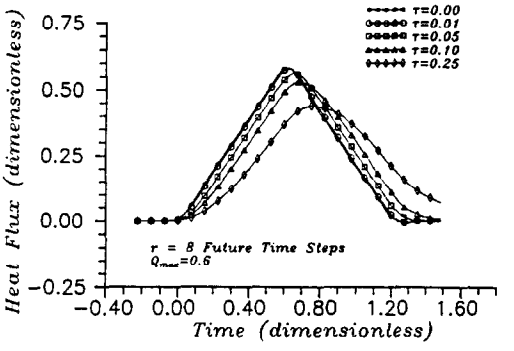

FIG. 8. Effect of τ on IHC surface heat flux predictions.

Figure 6 shows the result of the computations. In the figure, the case $\tau = 0$ corresponds to the case of no effect of sensor dynamics (perfect thermal contact or zero sensor heat capacity) and is thus the true temperature of the body. As the time constant is increased, the sensor lags progressively behind the true temperature.

These computed thermocouple responses were saved for input into the IHC algorithm to determine the effect of τ on the predicted surface heat flux. The results of this exercise, being the primary purpose of this paper, are presented in the next section.

4. EFFECT OF THERMOCOUPLE DYNAMICS ON IHC PREDICTIONS

To determine the effect of the thermocouple sensor dynamics on the IHC predictions, the results of the previous section's simulation of a sensor located at $x^+ = L$ were analyzed using the IHC algorithm described previously. The IHC analysis provides estimates of both the surface temperature and the surface heat flux. These results will be presented, followed by a study of the effect of the rate of heat flux change $d\dot{q}''/dt$ on the IHC predictions.

4.1. *Surface temperature*

The results of the IHC prediction of surface temperature for several different values of τ are shown in Fig. 7. Also shown in the figure are the actual values of surface temperature produced from the Crank–Nicolson simulation. The case of $\tau = 0$, corresponding to the case of no sensor dynamics or perfect readings, is seen to be faithfully reproduced by the IHC results in Fig. 7.

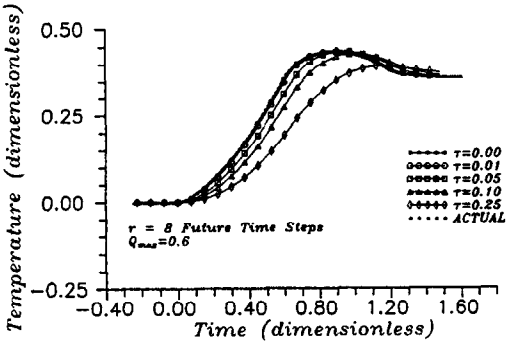

FIG. 7. Effect of τ on IHC surface temperature predictions.

As expected, increasing the parameter τ results in increasing error in the estimated surface temperatures. The nature of this error is a combination of a progressing shift in time of the response and a damping in the magnitude. These factors result from the cummulative effects of the lagging sensor response. When the time constant is degraded to $\tau = 0.25$, the IHC algorithm fails to predict the 'overshoot' in the surface temperature resulting from the triangular heat flux in Fig. 1.

4.2. *Surface heat flux*

The primary function of the IHC analysis is to estimate the surface heat flux based on the internal sensor temperature. The results of the IHC predictions of surface heat flux for several different sensor time constants τ are shown in Fig. 8. Again, the case of $\tau = 0$ corresponds to the estimate for a perfect sensor, and its error (depicted in Fig. 4) is indicative of the amount of error inherent in the IHC algorithm.

In Fig. 8, increasing values of τ produce increased damping and lagging of the surface heat flux predictions. This is analogous to damping and lagging of the predictions of surface temperature presented above. The lagging of the occurrence of the peak in the curve is seen to correspond approximately to the value of the time constant for the sensor. The magnitude of the peak flux predicted by the IHC degrades rapidly with the sensor's time constant τ.

4.3. *Effect of rate of change of heat flux on the IHC predictions*

The previous sections have considered the effects of using progressively inferior thermocouples to measure the temperature of a slab subjected to an identical heat flux history. In this section, the more physically realistic case is considered, that being a study of the effect of progressively steeper heat flux gradients $d\dot{q}''/dt$ on a thermocouple with a fixed time constant.

To achieve this comparison, a thermocouple with a

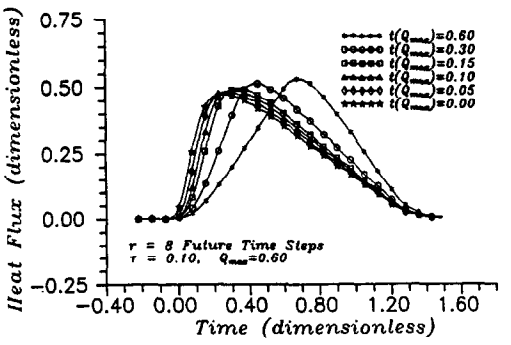

FIG. 9. Effect of heat flux gradient on IHC predictions with $\tau = 0.10$.

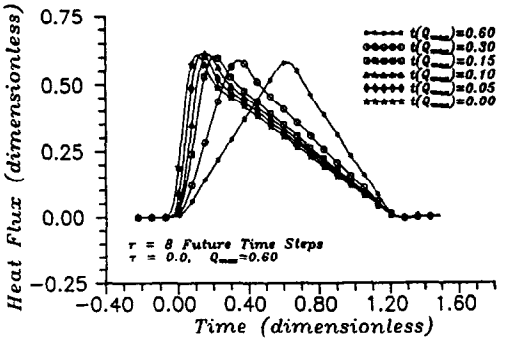

FIG. 10. Effect of heat flux gradient on IHC predictions with $\tau = 0.0$.

fixed parameter of $\tau = 0.10$ was selected. Such a thermocouple has a noticeable, but not catastrophic, effect on the IHC predictions seen in Figs. 7 and 8. The thermocouple's response was simulated, as described previously, being excited by a triangular heat flux similar to that in Fig. 1. On each successive simulation, the time at which the heat flux reaches its maximum value ($Q_{max} = 0.6$) was decreased until, for the last case, $t(Q_{max}) = 0.0$ which corresponds to an instantaneous change in surface heat flux.

The results of the IHC predictions of surface heat flux are shown in Fig. 9. For all six cases shown, the time at which the heat flux began increasing was fixed at $t = 0$, and the time at which the heat flux returned to zero was fixed at $t = 1.2$. The magnitude of the maximum heat flux was constant at $Q_{max} = 0.6$. As the time at which Q_{max} is reached is decreased, the rate of increase of the heat flux, $d\dot{q}''/dt$, increases. Initially, when $t(Q_{max}) = 0.60$, $d\dot{q}''/dt = 1.0$, and when $t(Q_{max})$ is decreased to zero, $d\dot{q}''/dt$ becomes infinite.

In Fig. 9, it is seen that as the rate $d\dot{q}''/dt$ increases, the heat flux predicted by the IHC algorithm is diminished in magnitude and delayed in time. The amount of the effect seen in Fig. 9 which is due to the thermocouple sensor dynamics can be ascertained by comparison with the results of the same analysis with a perfect temperature sensor. The results of this analysis are seen in Fig. 10. In this case, as $d\dot{q}''/dt$ increases, the peak values of the heat flux are actually overestimated, due to the inclusion of the future data information in the estimation procedure. Also, the time of occurrence of the peak values is closer to the actual value, but still is biased due to the inclusion of future time step information in the IHC prediction. Lastly, as the heat flux decreases from its maximum value, an irregularity in the shape of the triangle becomes apparent as $d\dot{q}''/dt$ is increased.

The essential details of Figs. 9 and 10 are tabulated in Table 2. There a comparison of the magnitude (Q_{max}) and time of occurrence ($t(Q_{max})$) of the maximum heat flux for the perfect and imperfect thermocouple sensors is made. As $d\dot{q}''/dt$ increases, the error in the predicted time of occurrence increases for both cases. In the perfect sensor case, this error is indicative of the inherent error in the IHC algorithm for the combination of the number of future time steps used ($r = 8$) and the time step in the data ($\Delta t = 0.015$). In the imperfect sensor, the error in the predicted time of occurrence is increased beyond that for the perfect sensor in all but the first case. The predicted magnitude of the maximum heat flux Q_{max} actually increases with increasing $d\dot{q}''/dt$ for the perfect sensor case, due to the use of future time step information. In the case of the imperfect sensor, the predicted magnitude of Q_{max} is steadily deteriorated with increasing $d\dot{q}''/dt$.

5. PROSCRIPTION FOR COMPENSATION OF THE IHC ALGORITHM FOR THERMOCOUPLE DYNAMICS

The deterministic effects of thermocouple sensor dynamics on predictions by IHC methodology were

Table 2. Comparison of IHC predictions for increasing heat flux gradients for perfect ($\tau = 0.0$) and imperfect ($\tau = 0.10$) sensors

	Actual		$\tau = 0.0$		$\tau = 0.10$	
$d\dot{q}''/dt$	Q_{max}	$t(Q_{max})$	Q_{max}	$t(Q_{max})$	Q_{max}	$t(Q_{max})$
1.0	0.60	0.60	0.5798	0.615	0.5278	0.615
2.0	0.60	0.30	0.5876	0.345	0.5108	0.435
4.0	0.60	0.15	0.6027	0.210	0.4941	0.330
6.0	0.60	0.10	0.6112	0.165	0.4872	0.300
12.0	0.60	0.05	0.6144	0.135	0.4800	0.270
∞	0.60	0.00	0.6084	0.105	0.4716	0.255

demonstrated in the previous section. It would be highly desirable, if possible, to account for the sensor's dynamics in the IHC method.

This can be done if the thermocouple can be modeled as the simplest case presented, i.e. the thermocouple's dynamics can be characterized by a single value τ. If the value of τ is known a priori, and is truly constant, then it is a trivial matter to include in the thermal model of the IHC algorithm a separate module to reflect this.

However, in the more general case, a suitable value of τ is *not* known. As mentioned before, this parameter depends on the *in situ* characteristics of the thermocouple bead and its contact condition with the surrounding body. The value of τ may even change during the experiment under consideration, owing to the (possibly) changing contact condition.

If the value of τ is not known, it can, under certain conditions, be estimated in parallel with the surface heat flux. This will require inclusion of the thermocouple dynamics in the IHC thermal model, leaving τ as an unknown function of time. The algorithm will now require more data, however, as the data from a single sensor will not be sufficient to determine two parameters at each time step. This would be analogous to the case mentioned earlier of attempting to determine the heat flux from two surfaces using data from a single sensor. The internally computed sensitivity coefficients will be competing for information from a single sensor's data. The parameter which is most dependent on the measured temperature will prevail, and the other parameter will be estimated as zero. If data from a second sensor is available, *and it can be assumed that the two sensors have similar dynamics*, then the algorithm can be modified to predict both the unknown surface heat flux *and* the unknown value of τ.

6. CONCLUSIONS

The effect of thermocouple sensor dynamics on predictions from IHC methods has been demonstrated. As one would expect, the 'slower' the sensor is, the poorer will be the results of the IHC method. The effect of increasing heat flux gradient $d\dot{q}''/dt$ on the IHC predictions from an imperfect sensor have also been illustrated. With a sensor of non-zero τ, as $d\dot{q}''/dt$ is increased, the times of occurrence and magnitudes of the peak values of heat fluxes are delayed and diminished.

REFERENCES

1. A. Markovsky and T. F. Soules, Application of inverse theory to viscoelasticity: evaluation of warpage and thermal stresses in viscoelastic–elastic composites. In *Inverse Design Concepts and Optimization in Engineering Sciences* (Edited by G. S. Dulikravich), pp. 337–350, 26–28 October (1987).
2. G. M. L. Gladwell, Inverse problems in structural vibration. In *Inverse Design Concepts and Optimization in Engineering Sciences* (Edited by G. S. Dulikravich), pp. 551–564, 26–28 October (1987).
3. M. F. Zedan, A. A. Seif and Y. O. Al-Hukail, The modification of a torpedo by the inverse method for reduced drag. In *Inverse Design Concepts and Optimization in Engineering Sciences* (Edited by G. S. Dulikravich), pp. 227–250, 26–28 October (1987).
4. A. Moutsoglou, An inverse convection problem, *Trans. ASME J. Heat Transfer* **111**, 37–43 (February 1989).
5. J. V. Beck, Nonlinear estimation applied to the nonlinear inverse heat conduction problem, *Int. J. Heat Mass Transfer* **13**, 703–716 (1970).
6. N. M. Al-Najem and M. N. Özisik, Inverse heat conduction in composite layers. ASME Preprint 85-HT-53, American Society of Mechanical Engineers, 4–7 August (1985). Presented at 24th National Heat Transfer Conference.
7. M. E. Irving, Boiling curves of liquid nitrogen obtained on spheres by the quenching method. Ph.D. thesis, University of Illinois at Urbana–Champaign, Urbana, Illinois (March 1986).
8. N. Zabaras, S. Mukerjee and O. Richmond, An analysis of inverse heat transfer problems with phase changes using an integral method, *Trans. ASME J. Heat Transfer* **110**, 554–561 (1988).
9. J. V. Beck, Combined parameter and function estimation in heat transfer with application to contact conductance, *Trans. ASME J. Heat Transfer* **110**, 1046–1058 (November 1988).
10. J. V. Beck, B. Blackwell and C. St. Clair, *Inverse Heat Conduction: Ill-posed Problems*. Wiley-Interscience, New York (1985).
11. J. L. Junkin, *An Introduction to Optimal Estimation of Dynamical Systems*, pp. 29–41. Sijthoff and Noordhoff, The Netherlands (1978).
12. J. V. Beck and K. J. Arnold, *Parameter Estimation in Engineering and Science*, pp. 340–361. Wiley, New York (1977).

EFFET DE LA DYNAMIQUE D'UN CAPTEUR THERMOCOUPLE SUR LA PREDICTION DU FLUX THERMIQUE OBTENUE PAR LA METHODE INVERSE

Résumé—Un modèle simple de thermocouple est utilisé pour simuler l'histoire successive à l'imposition, sur un domaine monodimensionnel, d'un flux thermique variant en triangle. Un programme d'informatique d'analyse inverse de conduction thermique est développé pour estimer l'évolution du flux après cette imposition. Les résultats montrent que l'effet de la constante du thermocouple est de diminuer l'intensité du flux estimé et de décaler sa distribution dans le temps.

DER EINFLUSS DES DYNAMISCHEN VERHALTENS VON THERMOELEMENTEN AUF DIE ERMITTLUNG DER OBERFLÄCHENWÄRMESTROMDICHTE DURCH DIE ANALYSE DER INVERSEN WÄRMELEITUNG

Zusammenfassung—In dieser Arbeit wird ein einfaches Modell eines Thermoelementes verwendet, um in einem eindimensionalen Gebiet die zeitliche Entwicklung der Wärmeströme zu berechnen. Es wird ein allgemeingültiges Rechenprogramm für die inverse Wärmeleitung entwickelt und dazu verwendet, aufgrund der generierten Daten die zeitliche Entwicklung des Wärmestroms zu berechnen. Die Ergebnisse zeigen, daß infolge der Zeitkonstanten des Thermoelementes die Wärmeströme betragsmäßig zu klein und im übrigen zeitversetzt berechnet werden.

ВЛИЯНИЕ ДИНАМИЧЕСКОЙ ХАРАКТЕРИСТИКИ ТЕРМОПАРЫ НА ОПРЕДЕЛЕНИЕ ТЕПЛОВОГО ПОТОКА НА ПОВЕРХНОСТИ С ИСПОЛЬЗОВАНИЕМ МЕТОДОВ РЕШЕНИЯ ОБРАТНЫХ ЗАДАЧ ТЕПЛОПРОВОДНОСТИ

Аннотация—Используется простая модель термопары для получения данных путем моделирования наложения на одномерную область теплового потока, распределенного во времени по треугольной схеме. Для восстановления теплового потока по результатам измерения разработана программа численного счета, основанная на решении обратных задач теплопроводности. Численный эксперимент показывает, что влияние постоянной времени заключается в сглаживании и смещении величины теплового потока во времени.